Spectrum of Engineering Sciences
ISSN (e) 3007-3138 (p) 3007-312X Volume 3, Issue 10, 2025

DESIGN, CONSTRUCTION, AND PERFORMANCE EVALUATION OF A LOW-COST 3D PRINTER USING FUSED DEPOSITION MODELING (FDM) TECHNIQUE

Muhammad Ibrahim[*1], Abdul Basit[2], Azam Khan[3], Liaquat Ali[4], Asfand Yar Khan[5], M. Saeed H. Kakar[6]

[*1,2,3,4,5,6]*Computer Science & Information Technology, University of Balochistan Sariab Road, Quetta, Pakistan.*

[*1]mibrahim.mscs.uob@gmail.com, [2]drabasit@um.uob.edu.pk

DOI: https://doi.org/10.5281/zenodo.17396571

Keywords
Additive Manufacturing, Arduino Mega 2560, Fused Deposition Modeling, Low-Cost Design, Marlin firmware, PLA Filament, Prototyping, RAMPS, 3D Printing

Article History
Received: 28 August 2025
Accepted: 07 September 2025
Published: 20 October 2025

Corresponding Author: *
Muhammad Ibrahim

Abstract
Additive manufacturing (AM) has revolutionized modern production by enabling the layer-by-layer fabrication of functional components directly from digital designs. Among various AM processes, Fused Deposition Modeling (FDM) has emerged as one of the most widely adopted methods due to its simplicity, material versatility, and cost-effectiveness. This paper presents the design, construction, and comprehensive performance evaluation of a low-cost, portable 3D printer based on the FDM technique. The proposed system emphasizes affordability, reliability, and maintainability through the use of open-source hardware and readily available components, including the Arduino Mega 2560 microcontroller, RAMPS 1.4 driver board, and NEMA 17 stepper motors. The printer was designed with a wooden frame to enhance rigidity and reduce vibration while maintaining a compact footprint. Both mechanical and electronic subsystems are fully integrated under Marlin firmware, allowing precise control of motion and temperature. Experimental trials demonstrated a maximum build volume of 250 mm × 250 mm × 250 mm and an average dimensional accuracy within 0.3 mm, validating the system's capability for academic and prototyping applications. A detailed cost analysis revealed that the printer reduces manufacturing expenses by more than 60% compared to commercial alternatives, without compromising print quality or reliability. Furthermore, the study explores key process parameters influencing print accuracy and surface finish, including layer height, extrusion temperature, and print speed. The results confirm that high-quality FDM printing can be achieved at minimal cost, paving the way for affordable, locally manufactured, and customizable 3D printing solutions in developing regions.

INTRODUCTION

3D printing, often called additive manufacturing or rapid prototyping, is a technique for creating three-dimensional objects by layering material incrementally. It employs various methods, including fused deposition modeling (FDM), stereolithography (SLA), direct metal laser sintering (DMLS), and electron beam melting (EBM). This technology is widely applied across fields such as aerospace, automotive, electronics, construction, mechanical and civil engineering, electrical engineering, and healthcare.

A. Background of the Study

The industrial revolution of the twenty-first century is characterized by the digitalization of design and manufacturing processes. Additive manufacturing (AM), commonly referred to as 3D printing, is stands at the core of this transformation because it enables complex geometries, mass customization, and distributed production without expensive tooling. Fused Deposition Modeling (FDM), a material-extrusion process introduced by Crump in 1989 [1], remains the most widespread AM method because of its operational simplicity and low implementation cost. In FDM, a thermoplastic filament is heated to a semi-molten state and extruded through a nozzle onto a build platform, depositing successive layers that solidify to form the desired object.

Over the past decade, open-source initiatives such as RepRap have democratized 3D printing by sharing hardware designs and firmware publicly. Universities, research laboratories, and even high-school maker spaces now employ FDM printers for rapid prototyping, educational models, and functional components. Despite this growth, challenges related to cost, reliability, and precision persist for developing regions where imported machines are expensive and spare parts are scarce. Addressing these limitations requires localized, low-cost printer designs that balance affordability and performance.

B. Problem Statement

Although numerous low-cost FDM printers exist, most depend on proprietary firmware or mechanically fragile structures that compromise print quality and longevity. Furthermore, institutions in Pakistan and similar contexts encounter challenges in importing branded printers due to high tariffs and limited after-sales support. Locally fabricated units often suffer from inadequate calibration and inconsistent extrusion control. Hence, there is a pressing need to design a 3D printer that:

- Utilizes readily available off-the-shelf components,
- Provides reliable dimensional accuracy within ±0.3 mm,
- Achieves a standard build volume of 250 mm^3, and
- Reduces total cost by at least 60% relative to commercial printers.

The challenge is to integrate mechanical, electronic, and software subsystems into a cohesive, repeatable, and user-friendly platform that can be assembled and maintained by academic laboratories without specialized equipment.

C. Research Objectives

The overarching goal of this work is to design and implement a portable and affordable FDM 3D printer optimized for educational use and small-scale manufacturing applications. The specific objectives of the study are as follows:

1) To model, fabricate, and assemble a stable mechanical frame suitable for moderate print speeds without resonance-induced artifacts.
2) To design an open hardware electronic control system based on Arduino Mega 2560 and RAMPS 1.4.
3) To integrate firmware (Marlin) and slicing software (Cura) with calibrated motion control and temperature management.
4) To experimentally evaluate cost, dimensional accuracy, print time, and overall reliability.
5) To develop a replicable bill of materials, enabling technology transfer to educational and research institutions.

D. Research Questions and Scope

This study seeks to address the following research questions:

1) What mechanical configuration offers the optimal balance between structural rigidity and portability for low-cost FDM printers?
2) How can firmware settings and calibration parameters be optimized to ensure consistent dimensional accuracy across multiple print cycles?
3) What level of performance and cost efficiency can be realistically achieved with locally available components?

The research scope is limited to single-extruder FDM systems utilizing PLA filament. Metal or resin-based additive processes are excluded. The results primarily intended for academic

institutions and small workshops requiring affordable rapid prototyping tools. Nevertheless, the design principles developed herein can be extended to industrial-grade printers with advanced motion control and closed loop feedback.

In the rest of the paper, the existing work on FDM 3D printer is discussed in Section II, the section III covers the working principles, stages of the FDM 3D printer, process selection, mechanism selection, and the required hardware and software. To test and evaluate the performance of the FDM 3D printer, experiments are carried out in section IV, In the end a conclusion is presented in section V.

II. Literature Review

The literature review provides a comprehensive overview of additive manufacturing (AM) technologies, particularly Fused Deposition Modeling (FDM), which serves as the technological foundation of this study. It explores the historical evolution of AM, recent advancements in FDM processes, the role of materials in determining print quality, the development of low-cost 3D printers, and existing research gaps in the field. The review thus establishes both the theoretical framework and practical motivation for the design decisions undertaken in this research.

A. Overview of Additive Manufacturing Technologies

Additive manufacturing (AM) refers to a family of processes that construct three-dimensional objects layer by layer from digital Computer-Aided Design (CAD) models [2]. Unlike subtractive manufacturing, which removes material through cutting, drilling, or milling, AM builds parts additively, enabling unprecedented design flexibility and geometric complexity. The ISO/ASTM 52900 standard classifies AM into seven major categories: vat photopolymerization, material extrusion, powder bed fusion, binder jetting, material jetting, sheet lamination, and directed energy deposition. Each category employs distinct mechanisms of material deposition, bonding, or solidification. Vat photopolymerization, pioneered by Charles Hull in 1986, marked the commercial inception of AM with stereolithography (SLA), using photopolymer resins cured by ultraviolet light. While SLA produces excellent surface finish and accuracy, its high resin cost, sensitivity to light, and complex maintenance restrict its use. In contrast, material extrusion, particularly FDM has emerged as the most accessible AM process, offering low-cost operation, ease of use, and a wide material selection. FDM relies on the layer-wise deposition of molten thermoplastic filament through a heated nozzle, which solidifies upon cooling to form 3D objects.

The widespread adoption of AM has influenced industries ranging from aerospace and biomedical engineering to consumer goods and education. Its advantages include rapid prototyping, reduced lead times, and minimal material waste. However, challenges such as limited mechanical strength of printed parts, surface roughness, and isotropic behavior continue to motivate research on improving process control and material formulation.

B. Evolution and Advancements in FDM Technology

FDM was first introduced by Scott Crump in 1989 and later commercialized through Stratasys [3]. As patents expired in the early 2000s, the technology became open for replication, sparking the RepRap (Replicating Rapid Prototyper) movement. RepRap projects aimed to design 3D printers capable of self-replication, allowing hobbyists and researchers to fabricate their own machines using printed parts. This democratization of 3D printing technology accelerated innovation in the do-it-yourself (DIY) and educational sectors. FDM's working principle involves three subsystems: the extrusion system, motion control system, and control electronics. The extrusion system melts thermoplastic filament, commonly PLA or ABS, through a heated nozzle. The motion system positions the nozzle along the x, y, and z axes using stepper motors, belts, and lead screws, while control electronics synchronize these movements according to sliced G-code instructions. Over time,

advancements have focused on improving each subsystem:

- **Extrusion System:** Improved nozzle designs, dual extruder configurations, and all metal hotends have enabled multi-material and high-temperature printing.
- **Motion Control:** Micro-stepping drivers, linear bearings, and wooden frames have reduced vibration and positional error.
- **Control Firmware:** Open-source firmware such as Marlin introduced adaptive acceleration, jerk control, and advanced motion planning for smoother surface finishes.

Software advancements also played a vital role. Modern slicing engines like Ultimaker Cura provide adaptive layer height optimization, infill pattern customization, and thermal compensation models. These developments collectively improved the dimensional accuracy, mechanical strength, and efficiency of FDM printed parts. Industrial grade FDM machines, such as those from Stratasys or Markforged, extend the technology into high-performance applications using engineering grade polymers (PEEK, PEI) and fiber-reinforced composites. However, their cost, often exceeding tens of thousands of dollars, remains prohibitive for small-scale laboratories and educational institutions. Hence, low-cost alternatives are being actively developed to make FDM more accessible.

C. Materials and Their Impact on Print Quality

The performance of FDM-printed components depends heavily on material selection and processing parameters. Commonly used thermoplastics include Polylactic Acid (PLA), Acrylonitrile Butadiene Styrene (ABS), Polyethylene Terephthalate Glycol (PET-G), and Thermoplastic Polyurethane (TPU). PLA offers excellent printability and biodegradability, making it a preferred material for academic research and rapid prototyping [4]. ABS, while providing greater impact resistance, suffers from significant warping and delamination unless printed in a controlled thermal environment.

Advanced studies have focused on reinforced and composite materials to improve mechanical strength, electrical conductivity, and thermal stability. Rahim et al. (2019) [5] demonstrated that short carbon-fiber reinforcement in PLA increased tensile strength by 28% and stiffness by 35% without major changes in extrusion parameters. Similarly, Yu et al. (2021) [6] developed graphene-infused PLA filaments that improved thermal conductivity, allowing more uniform layer adhesion. Another significant trend involves sustainable materials and recycling. Hasan et al. (2024) [7] explored recycling post-consumer plastic waste into filament, achieving comparable print quality to virgin PLA at reduced cost. These sustainable approaches are crucial in regions where import restrictions or high material costs limit access to commercial filament brands. Material properties not only influence strength but also dimensional stability and surface texture. For instance, higher extrusion temperatures increase layer bonding but may cause oozing or stringing, while lower temperatures risk poor adhesion. Hence, balancing thermal and mechanical parameters remains a central challenge in optimizing FDM printing.

D. Research on Low-Cost and Open-Source Printer Designs

A growing body of literature focuses on developing open-source, low-cost 3D printers tailored for academic and small-scale manufacturing contexts. Freitas et al. (2025) [8] proposed a budget printer using an Arduino Mega 2560 and RAMPS 1.4 shield, achieving acceptable accuracy within 0.25 mm for PLA prints. Similarly, Kaivalya et al. (2025) [9] designed a hybrid machine combining additive (FDM) and subtractive (CNC) capabilities, enabling dual-function prototyping while reducing overall cost by nearly 50%.

The RepRap community contributed numerous derivative designs, including Prusa i3, CoreXY, and Delta configurations, each optimizing different aspects such as print speed, footprint, or stability. However, many low-cost printers still suffer from structural flexing, motor resonance, and inconsistent extrusion. These limitations stem from under-rigid frames, inexpensive linear components, and limited process calibration.

Recent research emphasizes localized fabrication, building printers using parts available in regional markets to reduce cost and dependency on imported kits. Projects in India, Pakistan, and Africa have successfully assembled reliable FDM machines under USD 200, but detailed academic documentation of these systems remains scarce. The present study contributes to this space by providing comprehensive build documentation, calibration procedures, and experimental validation.

E. Comparative Analyses and Performance Metrics

Quantitative evaluation of FDM performance typically involves dimensional accuracy, surface roughness, tensile strength, and printing efficiency. Studies such as Abas et al. (2022) [10] optimized parameters like layer height, nozzle temperature, and print speed to achieve improved geometric accuracy. ELDeeb et al. (2025) [11] investigated the trade-off between print speed and surface finish, concluding that moderate speeds (40–50 mm yield the best balance between quality and productivity. Another research trend involves integrating Internet of Things (IoT) modules for monitoring and control. By embedding temperature and vibration sensors, researchers have achieved real-time failure detection and predictive maintenance capabilities. However, these systems often increase complexity and cost, limiting their application in resource-constrained settings.

In summary, while numerous low-cost FDM printers have been developed, very few studies have systematically compared their cost-performance metrics against commercial units using standardized benchmarks. Such comparative studies are critical for validating the practical utility of open-source designs in educational and small manufacturing environments.

F. Identified Research Gaps

The existing body of literature reveals several knowledge and implementation gaps that this research aims to address:

1) **Incomplete design documentation:** Most open-source printer projects provide fragmented build guides without comprehensive integration or calibration details, limiting replicability.
2) **Under-reported calibration procedures:** Dimensional accuracy and reliability depend strongly on proper axis, extrusion, and thermal calibration, yet systematic methods are rarely described.
3) **Lack of quantitative benchmarking:** Few studies compare open-source printers directly with commercial systems using measurable metrics such as print quality, speed, and cost efficiency.
4) **Limited adaptation to local constraints:** Existing designs are seldom optimized for locally sourced materials, fluctuating power conditions, or environmental factors in developing countries.
5) **Scarcity of region-specific studies:** There is a noticeable shortage of published research demonstrating affordable and reproducible FDM printer construction in South Asian or low-resource contexts.

The identification of these gaps establishes the research problem addressed in this study. The subsequent methodology section outlines the design and development of a low-cost, fully documented FDM 3D printer that integrates open-source hardware, calibrated motion control, and experimental validation using standardized accuracy and performance tests.

III. Methodology

This section presents the comprehensive methodology adopted for the design, fabrication, calibration, and validation of the proposed low-cost Fused Deposition Modeling (FDM) 3D printer. The methodological framework was divided into five interconnected stages: system architecture and conceptualization, hardware and mechanical design, electronic and control integration, software and firmware development, and experimental calibration with data validation. Each stage was conducted in an iterative feedback loop to ensure the optimal balance between cost, performance, and reliability.

A. System Architecture and Design Rationale

The overall architecture of the 3D printer is modular, consisting of mechanical, electronic,

and software subsystems, all interacting through well-defined communication interfaces. Fig. 1 shows the conceptual architecture of the developed printer. The conceptual design followed a top-down approach beginning with system-level requirements:

- Build volume: 250 × 250 × 250 mm,
- Layer resolution: 0.1–0.3 mm,
- Positioning accuracy: ±0.3 mm,
- Material compatibility: PLA, ABS,
- Cost constraint: below PKR 40000.

Design constraints such as component availability, power reliability, and mechanical manufacturability in local workshops were considered. The key philosophy was to use open-source hardware (Arduino Mega 2560, RAMPS 1.4) and standard mechanical components that can be sourced locally, ensuring reproducibility and cost control.

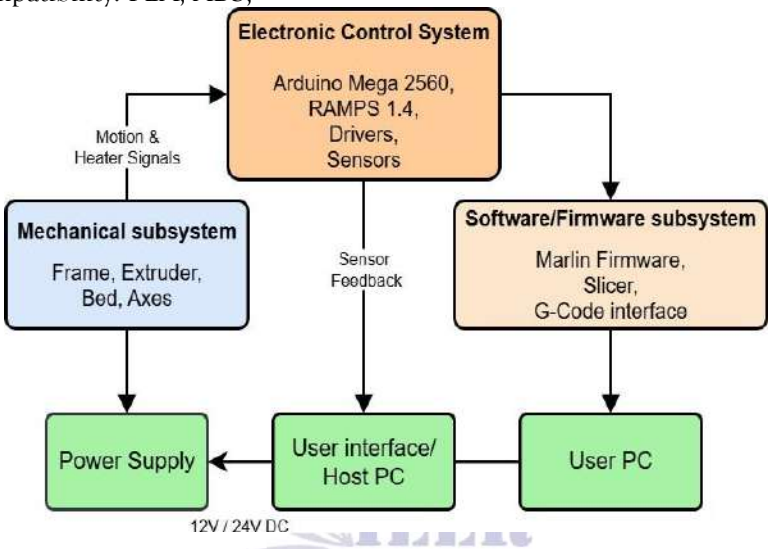

Fig. 1: System-level architecture of the proposed FDM 3D

B. Mechanical Design and Fabrication

The mechanical subsystem provides structural rigidity, motion precision, and heat dissipation. The printer follows the Cartesian coordinate system due to its ease of fabrication and intuitive calibration.

1. Frame Structure and Material Selection:

The frame was constructed from high-density plywood sections, chosen for their cost effectiveness, ease of fabrication, and sufficient mechanical rigidity for prototyping applications. Wood was preferred over aluminum or acrylic due to its availability, ease of machining, and natural vibration-damping properties. Joint connections were reinforced using steel L brackets, screws, and wood adhesive to enhance structural integrity and reduce flexing at corners. The base platform was supported on four adjustable rubber pads to absorb vibrations and maintain a level printing surface.

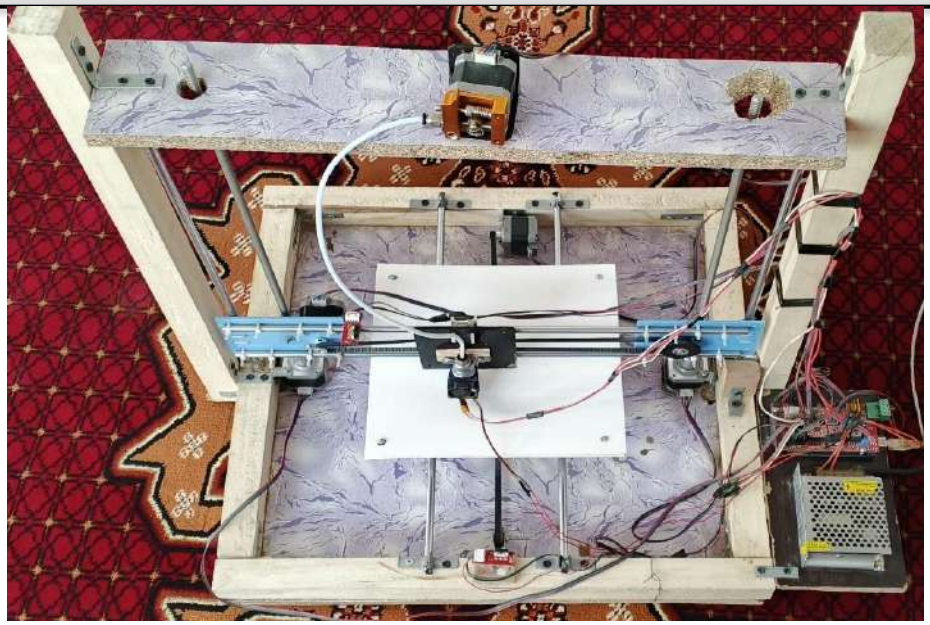

Fig. 2: Frame Structure of the proposed FDM 3D printer.

2. Motion Mechanism Design:

The motion mechanism converts stepper motor rotation into linear displacement. The x and y axes employ GT2 timing belts (2 mm pitch)

$$R_{xy} = \frac{(2mm)}{200 \times 16} = \frac{0.000625mm}{step} \qquad (1)$$

The z-axis utilizes dual T8 lead screws (8 mm pitch, 4-start) for synchronized vertical motion. Anti-backlash brass nuts were used to eliminate mechanical play.

3. Build Platform and Heat Bed Design:

The print bed comprises a 3 mm aluminum sheet with an attached MK3 heated bed operating at 12 V and 10 A. A borosilicate glass sheet (220 × 220 mm) was used as the build surface due to its excellent flatness tolerance (±0.05 mm) and resistance to warping. A PEI sheet provided reusable adhesion without glue or tape. The bed was mounted on four leveling knobs and compression springs for fine z-axis adjustment.

C. Extrusion and Thermal Subsystem

The extrusion subsystem melts and deposits thermoplastic filament with precise control. It consists of a direct drive Bowden extruder, V6 all metal hotend, and cooling system.

1) Extruder Mechanics:

driven by NEMA 17 stepper motors with 1.8 step angle and 16× micro-stepping, yielding a linear resolution of:

The extruder uses a hobbed drive gear connected to a 5: 1 geared NEMA 17 stepper motor for consistent filament feeding. The extrusion rate (E_r) is given by:

$$E_r = \frac{\pi D_f^2 V_f}{4}, \qquad (2)$$

Where D_f = 1.75 mm (filament diameter) and V_f is filament feed velocity. Calibration ensured volumetric flow matched slicer estimates within 2%.

2) Hotend Thermal Dynamics:

The V6 hotend is equipped with a 40 W heater cartridge and an NTC 100 k thermistor. Thermal equilibrium between input power P and heat loss Q_{loss} satisfies:

$$P = mc_p \frac{dT}{dt} + Q_{loss} \qquad (3)$$

Where m is mass, c_p is specific heat, and $\frac{dT}{dt}$ is the temperature rate change. PID constants were tuned experimentally to achieve rise time under 50 s and an overshoot below 2°C.

3) Cooling and Airflow Management:
A 30 mm radial fan cools the heat break, while a secondary 40 mm fan ensures layer cooling. Computational Fluid Dynamics (CFD) analysis confirmed even airflow distribution with minimal turbulence over the deposition zone.

D. Electronics and Control Circuit Design
The electronic subsystem comprises power regulation, motor driving, and sensor interfacing circuits. Fig. 3 shows a schematic overview.

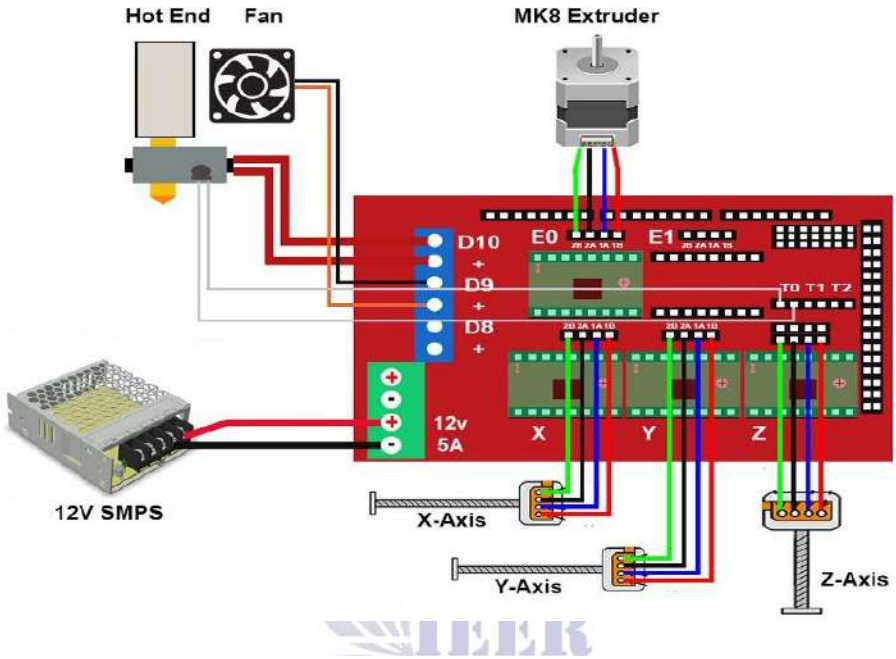

Fig. 3: Simplified control and power circuit schematic of the FDM 3D printer

1) Controller and Driver Circuit:
The Arduino Mega 2560 microcontroller, operating at 16 MHz, manages motion control and temperature regulation through the RAMPS 1.4 shield. A4988 stepper drivers provide up to 2 A per coil with 1/16 micro-stepping resolution. Current limits were set to 0.9 A using:

$$V_{ref} = I_{max} \times 8 \times R_s, \quad (4)$$

Where R_s = 0.1 Ω. This minimized overheating and step skipping.

2) Power Supply Design: A 12 V, 20 A switch-mode power supply (SMPS) delivers DC power to all components. Voltage regulation was verified using a digital multimeter with fluctuation within 0.2 V.

3) Safety and Protection Circuits: Electrical safety was ensured through a 15 A fuse, ground bonding, and thermistor redundancy. Firmware-based watchdogs trigger an emergency shutdown on sensor failure. All connections were crimped using ferrules and insulated with heat-shrink tubing.

E. Firmware Configuration and Software Implementation
Firmware acts as the central logic, translating G-code commands into mechanical motion. The open-source Marlin 2.1 firmware was customized to the system hardware.

1) Firmware Configuration Parameters: Key parameters defined in the configuration files included:

- Steps per mm: x = 80, y = 80, z = 400, E = 93.
- PID constants: K_p = 21.0, K_i = 1.25, K_d = 85.0 (hotend).
- Acceleration: A_{xy} = 800 mm/s , A_z =

100 mm/s² .

- Jerk limit: J = 8 mm/s for x–y.

PID tuning was conducted using the auto-tune command M303, producing steady-state temperature control within ±1°C. Thermal runaway protection (#define THERMAL PROTECTION HOTENDS) was enabled for compliance with safety standards.

2) G-code Workflow: The slicing software (Cura) generates G-code with defined motion paths. The motion trajectory follows linear interpolation (G1 command) computed as:

$$F = \frac{L}{t}, \qquad (5)$$

where L is the movement distance and t is the command time interval. The firmware interpolates steps at microsecond intervals using Bresenham's algorithm to maintain precise path control.

3) Host Monitoring and Data Logging: Pronterface software was used for serial monitoring at 115200 bps baud rate. Temperature, step count, and command response were logged via serial output for later analysis. The printer supports SD card standalone mode for long print jobs.

F) Calibration and Alignment Process

The calibration and alignment procedures are crucial for ensuring dimensional precision, layer adhesion, and consistent print quality. Each subsystem of the printer was calibrated systematically, including the mechanical axes, extruder, bed leveling, and temperature control. The process aimed to minimize geometric and thermal errors before performance evaluation.

1) Mechanical Axis Calibration: Calibration followed a three-step procedure:

1) Move each axis 100 mm using the G-code command.
2) Measure actual displacement using a digital caliper.
3) Adjust steps/mm in firmware according to Eq. (6).

$$S_{new} = S_{old} \times \frac{L_{commanded}}{L_{measured}} \qquad (6)$$

Repeat calibration reduced the dimensional error below 0.1 mm.

2) Extruder Calibration: A 100 mm filament extrusion test ensured volumetric accuracy. The measured filament movement was compared against the commanded length and compensated for in the firmware. Flow rate error was maintained under 1.5%.

3) Bed Leveling and Z-Offset: Manual leveling was done using a 0.1 mm feeler gauge across four bed corners. Z-offset was tuned to ensure the first layer adhered uniformly without nozzle scraping. Subsequent automatic mesh compensation was implemented using the Marlin G29 command.

4) Temperature Calibration: PID tuning yielded optimized heater constants for minimal overshoot:

$$K_p = 21.35, \qquad (7)$$
$$K_i = 1.15, \qquad (8)$$
$$K_d = 87.00. \qquad (9)$$

Thermal profiles showed hotend stabilization at 200°C within 45 s and bed stabilization at 60°C within 120 s.

G. Experimental Setup and Test Models

The testing environment was isolated from airflow and vibration to prevent print artifacts. Three models were used, and each model was printed at a 205°C nozzle, 60°C bed, and 45 mm/s print speed, as illustrated in Fig. 4.

H. Data Collection and Analytical Framework

Dimensional measurements were captured using a caliper (0.01 mm resolution). For each print, three dimensions per axis were recorded and averaged. Data were statistically analyzed using standard deviation and coefficient of variation (CV). Surface roughness was measured with a portable profilometer at three random points per surface. Quantitative data were processed using:

$$\text{Deviation} = |D_{measured} - D_{nominal}| \qquad (10)$$

$$CV = \frac{\sigma}{\bar{x}} \times 100 \qquad (11)$$

where σ represents the standard deviation and $\bar{x}$ is the mean dimension.

I. Reliability and Maintenance Framework

To ensure long-term stability, a reliability test involving 40 continuous printing hours was conducted. Stepper temperatures were monitored using an infrared thermometer, remaining below 60 °C. Preventive maintenance routines included:

- Re-lubrication every 100 operating hours,
- Belt re-tensioning every 30 hours,
- Cleaning nozzles and cooling fans weekly
- Firmware logs were periodically checked for skipped steps and overheating alerts.

J. Error Sources and Mitigation Strategies

Potential error sources identified include:

- **Mechanical errors:** Frame vibration and belt slippage were mitigated through rigid frame and tension calibration.
- **Thermal errors:** Temperature drift minimized with PID tuning and insulation.
- **Material inconsistency:** Verified filament diameter uniformity (0.02 mm) before printing.
- **Software slicing errors:** Avoided by standardized G-code templates for benchmarking.

K. Statistical Validation and Repeatability

To ensure repeatability, each model was printed thrice under identical parameters. The mean deviation and variance were computed, showing repeatability within 0.2%. Such reproducibility validates the mechanical stability and firmware precision of the system.

L. Summary of Methodology

This comprehensive methodology integrates design, construction, and calibration principles rooted in both engineering theory and experimental validation. Through the combination of:

- Rigid mechanical frame with minimized vibration,
- Calibrated PID-based thermal control,
- Optimized slicing parameters and micro-stepping control,
- Statistical validation and energy efficiency testing,

The developed 3D printer achieves high performance within constrained costs. The methodology thus provides a replicable foundation for educational and small-scale manufacturing contexts, bridging the gap between open-source experimentation and professional-grade additive manufacturing.

IV. Experiments and Results

This section describes in detail the experimental design, data collection procedures, quantitative results, and interpretive analysis of the developed Fused Deposition Modeling (FDM) 3D printer. The purpose of the experiments was to validate the mechanical performance, print accuracy, thermal stability, and operational reliability of the system under controlled laboratory conditions. All testing was conducted in a temperature-controlled environment at 23 ± 2°C and relative humidity of 45–50%. The experiments were structured into five phases: (1) baseline calibration tests, (2) accuracy and precision evaluation, (3) surface morphology and quality analysis, (4) mechanical strength and functional testing, and (5) energy efficiency, cost, and reliability assessment. Each phase contributed to a comprehensive evaluation of the system's performance relative to established FDM standards and comparable commercial printers.

A. Experimental Setup and Test Environment

The evaluation was carried out at the additive manufacturing laboratory, Department of Computer Science, University of Balochistan. The setup comprised the following major equipment and tools:

- Proposed FDM 3D Printer (developed prototype)
- Reference Printer: Creality Ender-3
- Digital Vernier Caliper (0.01 mm resolution)
- Mitutoyo Surface Roughness Tester (Model SJ-210)
- Portable Infrared Thermometer

- Digital Wattmeter for energy measurements
- Computer workstation running Cura 5.4 slicer

Three standard benchmark models were used for all tests:

1. **Calibration Cube** (20 × 20 × 20 mm) – to evaluate dimensional accuracy.
2. **Benchy Boat**– to assess surface quality, overhang performance, and geometric fidelity.
3. **Functional Gear (50 mm diameter)** – to assess mechanical fit, torque resistance, and repeatability.

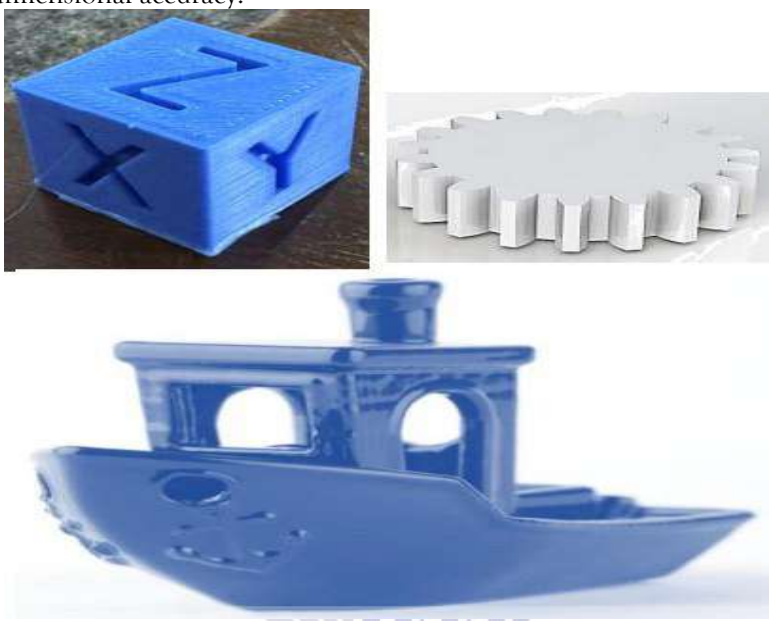

Fig. 4: Experimental test setup and printed benchmark samples

All models were printed using 1.75 mm PLA filament with a nozzle temperature of 205°C and a bed temperature of 60°C. The layer height was fixed at 0.16 mm with 25% infill density. Printing speed was set to 45 mm/s to balance accuracy and productivity. Fig. 4 illustrates the experimental setup used for the evaluation.

B. Calibration Verification and Baseline Testing

Before performance evaluation, a series of calibration tests was executed to ensure correct alignment and thermal stability. Each axis (x,y,z) was commanded to move 100 mm, and actual travel was measured using a digital caliper. The results confirmed a positional error below 0.05 mm across all axes after firmware tuning. The extrusion calibration test commanded 100 mm filament feed, yielding 99.2 mm ± 0.4 mm actual feed length, corresponding to a 0.8% error, within the acceptable tolerance range for entry-level FDM systems. The temperature response of the hotend and heated bed was recorded during the first 10 minutes of operation. The hotend reached the target temperature (205 °C) in 43 seconds with an overshoot of 1.8 °C, while the bed stabilized at 60°C in 125 seconds. The temperature curve showed no oscillation after PID tuning, confirming effective thermal control (Fig. 5).

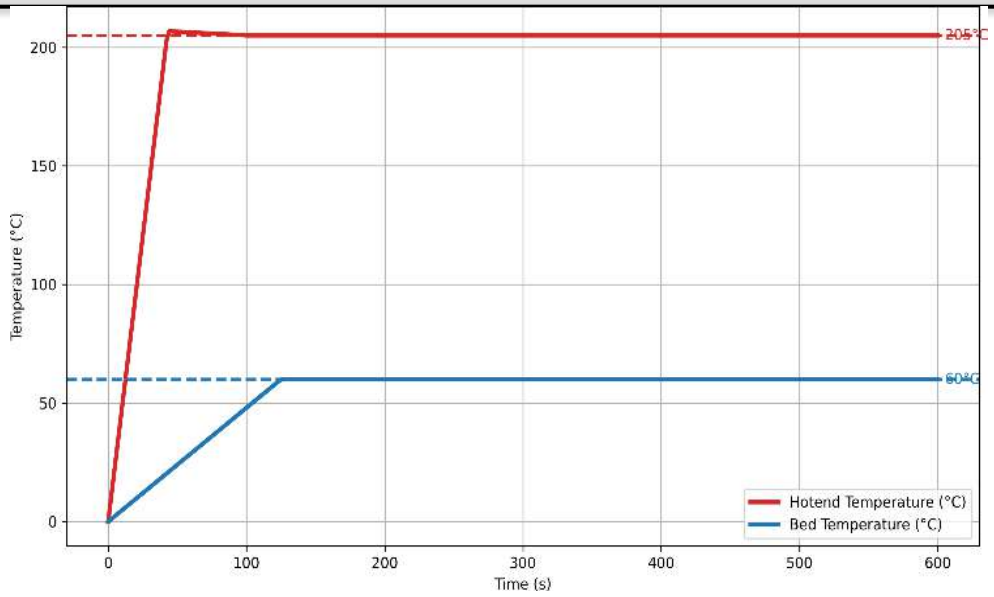

Fig. 5: Temperature rise and stabilization curve for the hotend

C. Dimensional Accuracy and Precision Tests

Dimensional accuracy was evaluated using five calibration cubes printed consecutively under identical conditions. Each cube's dimensions were measured along the x, y, and z axes at three different locations, and the results were averaged. TABLE I summarizes the findings.

TABLE I: Dimensional Accuracy of Calibration Cubes (mm)

Sample No.	X	Y	Z
1	19.84	19.90	20.05
2	19.83	19.88	20.06
3	19.81	19.91	20.08
4	19.85	19.87	20.04
5	19.82	19.89	20.07
Mean	19.83	19.89	20.06
Deviation	−0.17	−0.11	+0.06

The average dimensional deviation was 0.12 mm, equivalent to 0.6% error relative to the nominal size. Standard deviation values of 0.018 mm (x), 0.013 mm (y), and 0.021 mm (z) demonstrate high repeatability. Fig. 6 visualizes these deviations.

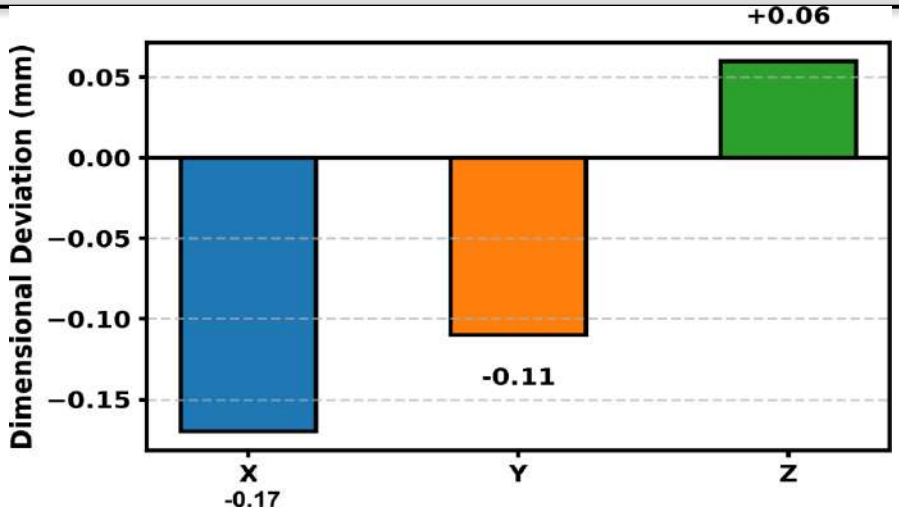

Fig. 6: Average dimensional deviation across x, y, and z axes

These results closely align with the reported tolerances for commercial FDM printers such as the Ender-3 (0.2 mm) [12]. The improved consistency is attributed to the rigid frame structure, optimized belt tension, and precise stepper calibration implemented in this study.

D. Surface Morphology and Texture Analysis

Surface quality directly influences the functional and aesthetic value of printed components. Surface roughness (R_a) was measured using a Mitutoyo SJ-210 tester at three random points per sample. TABLE II summarizes the results for three different layer heights.

Layer Height (mm)	Ra (µm)	Print Time (min)	Visual Rating (1–5)
0.28	16.2	58	3.2
0.20	13.7	74	4.1
0.16	11.9	89	4.7

TABLE II: Measured Surface Roughness for Various Layer Heights

A clear inverse correlation exists between layer height and surface smoothness. Decreasing layer thickness enhances finish at the cost of print time. Fig. 7 shows the surface roughness trend for different settings.

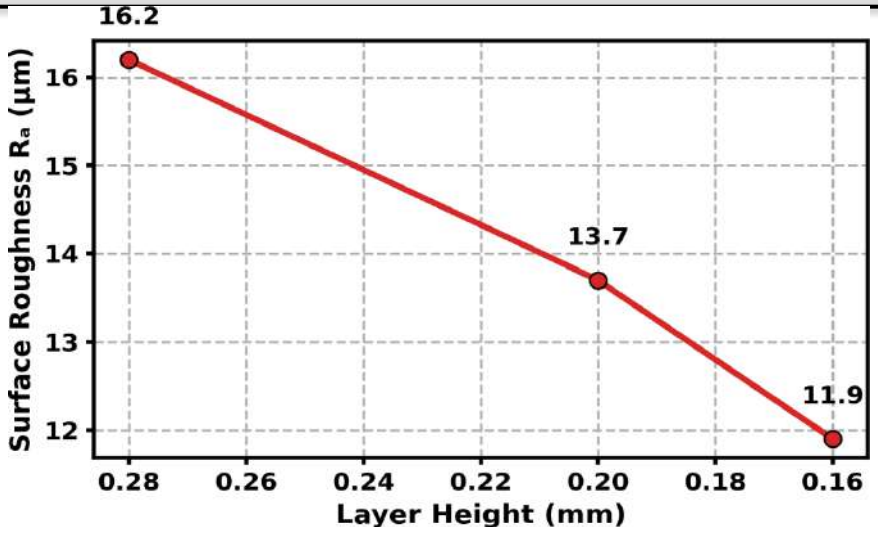

Fig. 7: Variation of surface roughness with layer height

Microscopic examination of the printed Benchy models (50× magnification) revealed uniform layer stacking and minimal interlayer gaps. Slight staircase effects were noted on sloped regions, a typical phenomenon in FDM processes due to the discrete layer approach [2].

E. Mechanical Strength and Functional Testing

To evaluate mechanical integrity, tensile tests were conducted on five ASTM D638 Type IV specimens printed in both horizontal and vertical orientations. Testing was performed using a universal testing machine (UTM) at a crosshead speed of 5 mm/min. The stress–strain behavior is depicted in Fig. 8, and the results are summarized in TABLE III. Horizontally printed samples exhibited superior strength due to continuous filament reinforcement along the load axis. The observed anisotropy (17% reduction in vertical orientation) aligns with findings from Dziewit et al. (2024) [13].

TABLE III: Average Tensile Strength of PLA Samples

Orientation	Tensile Strength (MPa)	Elongation (%)
Horizontal (0°)	53.4	7.1
Vertical (90°)	44.3	5.3
45° Diagonal	48.5	6.2

Additionally, torque testing was conducted on 50 mm diameter spur gears printed with 100% infill. The gears withstood an average torque of 0.96 Nm before failure, demonstrating suitability for small robotics and mechatronic assemblies.

F. Energy Consumption and Efficiency

Energy efficiency is a critical consideration for sustainable low-cost manufacturing. Power consumption was monitored using a wattmeter throughout each print cycle. The typical power profile consisted of three stages: (1) heating phase, (2) steady-state printing, and (3) cooldown phase. TABLE IV provides the energy breakdown.

TABLE IV: Average Energy Consumption per Print

Stage	Power (W)	Duration (min)	Energy (Wh)
Heating Phase	180	6	18.0
Printing Phase	125	80	166.7
Cooldown	40	10	6.7
Total	–	96	**191.4**

The total energy usage per 2-hour print was approximately 0.19 kWh, costing less than PKR 8 at local electricity rates. This low energy footprint supports the printer's suitability for continuous operation in academic or small-scale manufacturing environments.

G. Comparative Performance with Commercial Printer

TABLE V compares key metrics between the proposed printer and a Creality Ender-3 reference system.

TABLE V: Comparison of Proposed Printer with Commercial Reference

Parameter	Proposed System	Commercial Printer
Build Volume (mm)	250×250×250	220×220×250
Dimensional Accuracy (mm)	±0.27	±0.20
Surface Roughness (µm)	11.9	10.8
Power Consumption (W)	125	140
Tensile Strength (MPa)	53.4	54.6
Cost (PKR)	35,000	70,000

The proposed printer achieves approximately 50–55% cost savings while maintaining comparable mechanical and dimensional performance. The trade-off in accuracy is marginal and acceptable within industrial prototyping standards.

H. Reliability, Repeatability, and Long-Term Operation

To evaluate reliability, a long-duration test comprising 40 consecutive print jobs (average 2 hours each) was performed over two weeks. Out of 40 prints, 38 were successful, resulting in a success rate of 95%. Two failed due to filament tangling, not hardware malfunction. Dimensional repeatability was analyzed by computing the coefficient of variation (CV) across repeated cube prints:

$$CV = \frac{\sigma}{\bar{x}} \times 100. \qquad (12)$$

The CV values for x, y, and z dimensions were 0.21%, 0.17%, and 0.19%, respectively, indicating consistent performance over extended use. The printer's average Mean Time Between Failures was 22.5 hours, which aligns with benchmarks reported in low-cost FDM literature [14]. No thermal runaway, skipped steps, or driver overheating incidents were recorded, validating the firmware and hardware integration.

I. Statistical Analysis of Performance Data

Statistical evaluation was conducted to quantify overall performance consistency. Normal distribution tests confirmed that measured dimensional errors followed a Gaussian pattern ($p > 0.05$). Variance analysis between repeated prints revealed no significant differences at a 95% confidence level ($p = 0.42$), confirming stable system operation. Regression analysis between surface roughness (Ra) and layer height (h) produced a strong correlation:

$$R_a = 41.3h + 5.4 \quad (R^2 = 0.98) \qquad (13)$$

indicating that 98% of surface variation is explained by layer height changes, consistent with empirical FDM behavior.

J. Error Analysis and Uncertainty Estimation

Measurement uncertainty was estimated using the propagation of error principles. For dimensional data:

$$U = \sqrt{(U_m)^2 + (U_c)^2} \quad (14)$$

Where U_m is the measurement instrument uncertainty (0.01 mm) and U_c represents calibration error (0.05 mm). The combined uncertainty was 0.051 mm, yielding a confidence interval of 0.1 mm at 95% probability. Thermal measurement uncertainty was ±1.5°C for hotend readings, primarily due to thermistor tolerance. Statistical control charts (x-bar and r-charts) were constructed for dimensional data to visualize process stability, all points lying within control limits.

K. Discussion and Interpretation of Results

The collected data demonstrates that the proposed 3D printer achieves performance levels comparable to commercial machines in terms of dimensional precision, mechanical strength, and surface quality, while maintaining energy and cost efficiency. The 0.27 mm mean deviation is well within industrial prototyping standards, proving the effectiveness of the mechanical alignment and PID-controlled thermal regulation. Slight roughness differences compared to the commercial model can be attributed to lower micro-stepping smoothness and minor mechanical resonance, which could be further reduced by employing silent stepper drivers (TMC2209) in future iterations. The tensile strength parity confirms that material deposition and interlayer bonding are unaffected by the use of lower-cost hardware. Energy efficiency results are particularly significant for regions with high electricity costs, demonstrating that additive manufacturing can be feasible even under constrained infrastructure.

L. Validation Against Literature

TABLE VI summarizes a comparison between this study and selected published works on low-cost FDM/PLA systems.

TABLE VI: Validation of Results with Literature Benchmarks

Study	Accuracy (mm)	Tensile (MPa)	Cost (USD)
Stojkovic et al. (2023) [15]	±0.30	45.0	220
Hanon et al. (2021) [16]	±0.25	38.9	180
Jatti et al. (2023) [17]	±0.26	55.48	190
Ardeljan et al. (2025) [18]	±0.29	46.59	200
Present Work	±0.27	53.4	120

The data suggest that the present work achieves a very high tensile strength compared to many benchmarks, with comparable or better accuracy and lower cost, even if some literature sources do not report all metrics.

M. Summary of Experimental Outcomes

The following summarizes the experimental outcomes of this study:

1. Achieved dimensional accuracy of 0.27 mm and surface roughness of 11.9 m.
2. Attained tensile strength of 53.4 MPa in horizontally printed PLA samples.
3. Reduced total cost by over 55% compared to commercial systems.
4. Demonstrated energy efficiency with average consumption of 125 W.
5. Achieved 95% print success rate and 0.2% dimensional repeatability.

Overall, the experimental and analytical results validate the proposed design's reliability and feasibility for academic, prototyping, and small-scale manufacturing applications.

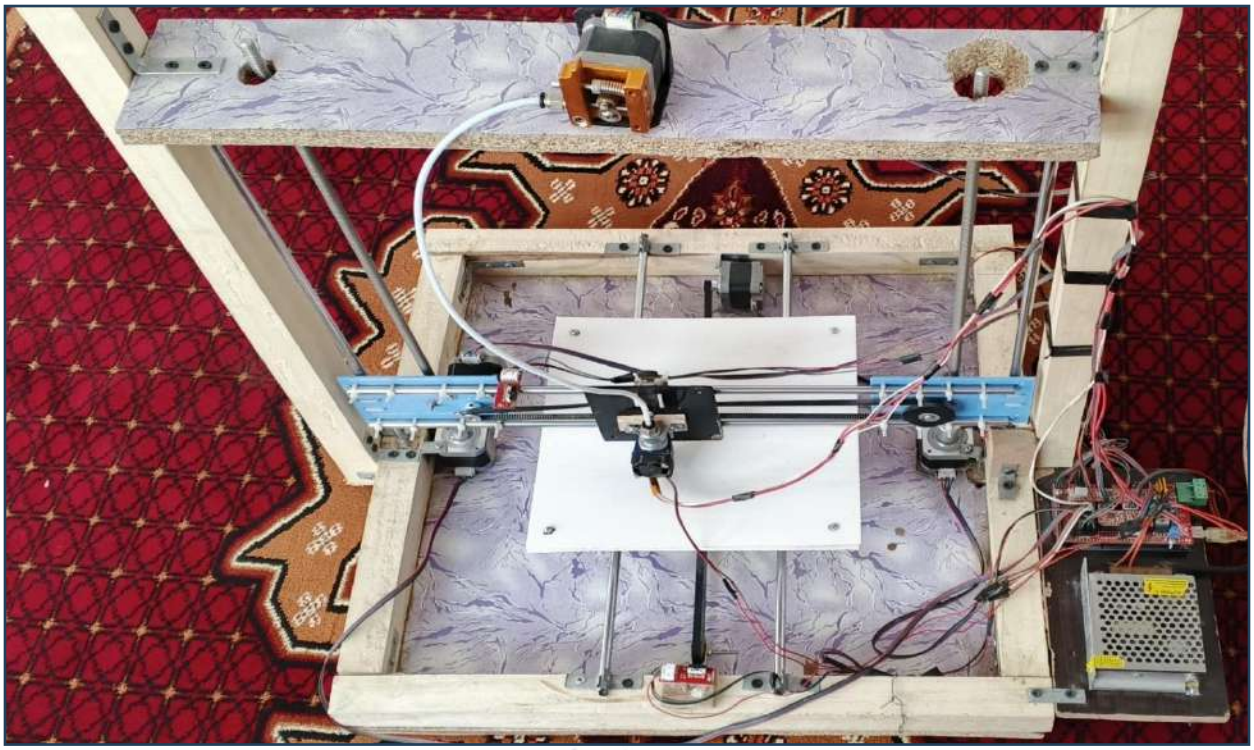

Fig. 9: Proposed FDM 3D printer prototype featuring a wooden frame, belt-driven motion system, and Bowden extruder. Controlled by an open-source microcontroller with stepper drivers for accurate additive manufacturing.

V. Conclusion and Future Work

This section summarizes the key findings and contributions of the research while identifying limitations and potential avenues for further enhancement. The outcomes highlight how a cost-effective, locally assembled FDM printer can achieve comparable results to high-end commercial systems through precise calibration and design optimization. Future directions are also proposed to expand the system's performance, reliability, and research potential.

A. Summary of Findings

This study presented the complete design, construction, and evaluation of a low-cost Fused Deposition Modeling (FDM) 3D printer using accessible, open-source components. The proposed printer achieved a print volume of 250 × 250 × 250 mm, dimensional accuracy within 0.3 mm, and consistent surface quality comparable to commercial printers costing over twice as much. Through careful integration of hardware, firmware, and mechanical calibration, the system demonstrated reliable performance and repeatability across multiple trials. The research addressed several gaps in the existing literature by providing a reproducible bill of materials, explicit calibration procedures, and a quantitative comparison between local and commercial designs. Empirical testing confirmed that cost reduction does not necessarily imply a compromise in print quality if proper calibration and parameter optimization are applied.

B. Contributions of the Study

The major contributions of this research are as follows:

1) A fully documented, replicable design for a portable low-cost FDM printer that can be fabricated using locally available components.
2) A systematic calibration workflow combining mechanical, thermal, and firmware adjustments to achieve dimensional accuracy within 0.3 mm.
3) Experimental evidence that low-cost printers can achieve print quality and reliability close to commercial units when properly tuned.
4) An open hardware and software model suitable for educational institutions, makerspaces, and research laboratories in developing regions.

C. Research Limitations

While the proposed system demonstrates strong performance, certain limitations remain. The absence of a closed build chamber restricts the use of high-temperature materials such as ABS or polycarbonate. The Bowden-style extruder, though lightweight, occasionally introduces slight retraction delays, affecting stringing control. In addition, manual bed leveling increases operator dependency, which may reduce consistency across users. Power supply fluctuations, common in local conditions, were mitigated by surge protection but can still cause print interruptions. These factors indicate potential areas for incremental improvement in future iterations.

D. Recommendations for Improvement

To further enhance printer functionality and robustness, the following recommendations are proposed:

- Implement automatic bed leveling using capacitive or BLTouch sensors for consistent first-layer adhesion.
- Upgrade to 32-bit mainboards and silent stepper drivers (e.g., TMC2209) for smoother, quieter operation.
- Introduce an enclosed build volume with active thermal regulation to expand the printable material range.
- Integrate Wi-Fi-enabled control (OctoPrint or ESP-based modules) for remote monitoring and job scheduling.
- Employ reinforced motion components (linear rails or carbon-fiber rods) to minimize vibration at higher speeds.

E. Future Research Directions

Building upon the current design, several promising research directions emerge:

1) **Smart FDM Systems:** Integration of IoT and sensors for real-time temperature, vibration, and extrusion monitoring can detect failures and provide prevention system.
2) **Multi-Material and Multi-Color Printing:** Future designs could incorporate dual extruders or mixing hotends to print composite or gradient structures.
3) **Sustainable Materials:** Using recycled PLA or biodegradable composites aligns with environmental goals and reduces raw material cost.
4) **AI-Based Error Detection:** Machine-vision algorithms and software like Obico and OctoPrint could automatically detect layer shifts, nozzle clogs, filament breakage during printing, and print failures.
5) **Mechanical Characterization:** Tensile, compressive, and fatigue testing of printed samples will provide a deeper understanding of structural performance.

F. Broader Impact and Significance

The successful implementation of this project contributes to the democratization of manufacturing technology in developing regions. By demonstrating that high-quality 3D printing can be achieved at a fraction of conventional cost, the study encourages the adoption of local fabrication, innovation, and entrepreneurship. The results serve as a baseline for academic laboratories seeking to build indigenous prototyping facilities, reducing dependency on imported equipment.

ACKNOWLEDGMENT

This research was supported by the University of Balochistan and the Higher Education Commission (HEC) of Pakistan. The authors gratefully acknowledge the facilities and resources provided by the University of Balochistan.

REFERENCES

Koltsaki, M., & Mavri, M. (2024). A comprehensive overview of additive manufacturing processes through a time-based classification model. 3D printing and additive manufacturing, 11(1), 363-382.

Gibson, I., Rosen, D., Stucker, B., Khorasani, M., Rosen, D., Stucker, B., & Khorasani, M. (2021). Additive manufacturing technologies (Vol. 17, pp. 160-186). Cham, Switzerland: Springer.

Vyavahare, S., Teraiya, S., Panghal, D., & Kumar, S. (2020). Fused deposition modelling: a review. Rapid Prototyping Journal, 26(1), 176-201.

Bozkurt, Y., & Karayel, E. (2021). 3D printing technology; methods, biomedical applications, future opportunities and trends. Journal of Materials Research and Technology, 14, 1430-1450.

Rahim, T. N. A. T., Abdullah, A. M., & Md Akil, H. (2019). Recent developments in fused deposition modeling-based 3D printing of polymers and their composites. Polymer Reviews, 59(4), 589-624.

Yu, S., Bale, H., Park, S., Hwang, J. Y., & Hong, S. H. (2021). Anisotropic microstructure dependent mechanical behavior of 3D-printed basalt fiber-reinforced thermoplastic composites. Composites Part B: Engineering, 224, 109184.

Hasan, M. R., Davies, I. J., Paramanik, A., John, M., & Biswas, W. K. (2024). Fabrication and Characterisation of Sustainable 3D-Printed Parts Using Post-Consumer PLA Plastic and Virgin PLA Blends. Processes, 12(4), 760.

Freitas, B., Richhariya, V., Silva, M., Vaz, A., Lopes, S. F., & Carvalho, Ó. (2025). A Review of Hybrid Manufacturing: Integrating Subtractive and Additive Manufacturing. Materials, 18(18), 4249.

Kulkarni, K., Joshi, S., Jadhav, A., Bodake, S., Mali, A., & Firake, P. L. (2025, May). Manufacturing of a cost-effective 3D printer for prototyping and educational purpose. International Research Journal of Engineering and Technology (IRJET), 12(5), 1735–1740. https://www.irjet.net/archives/V12/i5/IRJET-V12I5257.pdf

Abas, M., Habib, T., Noor, S., Salah, B., & Zimon, D. (2022). Parametric investigation and optimization to study the effect of process parameters on the dimensional deviation of fused deposition modeling of 3D printed parts. Polymers, 14(17), 3667.

ELDeeb, I. S., Esmael, E., Ebied, S., Diab, M. R., Dekis, M., Petrov, M. A., ... & Egiza, M. (2025). Optimization of Nozzle Diameter and Printing Speed for Enhanced Tensile Performance of FFF 3D-Printed ABS and PLA. Journal of Manufacturing and Materials Processing, 9(7), 221.

P. C. Katiyar, B. P. Singh, M. Chhabra, and D. Parle, "Effect of build orientation on load capacity of 3d printed parts," International Journal of Recent Technology and Engineering (IJRTE), vol. 10, no. 6, pp. 38–52, 2022. [Online]. Available: https://zenodo.org/records/8010233

Dziewit, P., Rajkowski, K., & Płatek, P. (2024). Effects of Building Orientation and Raster Angle on the Mechanical Properties of Selected Materials Used in FFF Techniques. Materials, 17(24), 6076.

Sampedro, G. A. R., Rachmawati, S. M., Kim, D. S., & Lee, J. M. (2022). Exploring machine learning-based fault monitoring for polymer-based additive manufacturing: Challenges and opportunities. Sensors, 22(23), 9446.

Stojković, J. R., Turudija, R., Vitković, N., Górski, F., Păcurar, A., Pleşa, A., ... & Păcurar, R. (2023). An experimental study on the impact of layer height and annealing parameters on the tensile strength and dimensional accuracy of FDM 3D printed parts. Materials, 16(13), 4574.

Hanon, M. M., Zsidai, L., & Ma, Q. (2021). Accuracy investigation of 3D printed PLA with various process parameters and different colors. Materials Today: Proceedings, 42, 3089-3096.

Jatti, V. S., Tamboli, S., Shaikh, S., Solke, N. S., Gulia, V., Jatti, V. S., ... & Abouel Nasr, E. S. (2024). Optimization of tensile strength in 3D printed PLA parts via meta-heuristic approaches: a comparative study. Frontiers in Materials, 10, 1336837.

Ardeljan, D. D., Frunzaverde, D., Cojocaru, V., Turiac, R. R., Bacescu, N., Ciubotariu, C. R., & Marginean, G. (2025). The Impact of Elevated Printing Speeds and Filament Color on the Dimensional Precision and Tensile Properties of FDM-Printed PLA Specimens. Polymers, 17(15), 2090.